Journal of Biological Engineering

RESEARCH Open Access

Enhancing fatty acid and omega-3 production in *Schizochytrium* sp. using developed safe-harboring expression system

Ae Jin Ryu[1†], Won-Sub Shin[1†], Sunghoon Jang[1], Yejin Lin[2], Yejee Park[2], Yujung Choi[2], Ji Young Kim[1*] and Nam Kyu Kang[2*]

Abstract

Background *Schizochytrium*, a group of eukaryotic marine protists, is an oleaginous strain, making it a highly promising candidate for the production of lipid-derived products such as biofuels and omega-3 fatty acids. However, the insufficient advancement of genetic engineering tools has hindered further advancements. Therefore, the development and application of genetic engineering tools for lipid enhancement are crucial for industrial production.

Results Transgene expression in *Schizochytrium* often encounters challenges such as instability due to positional effects. To overcome this, we developed a safe-harbor transgene expression system. Initially, the sfGFP gene was integrated randomly, and high-expressing transformants were identified using fluorescence-activated cell sorting. Notably, HRsite 2, located approximately 3.2 kb upstream of cytochrome c, demonstrated enhanced sfGFP expression and homologous recombination efficiency. We then introduced the 3-ketoacyl-ACP reductase (KR) gene at HRsite 2, resulting in improved lipid and docosahexaenoic acid (DHA) production. Transformants with KR at HRsite 2 exhibited stable growth, increased glucose utilization, and a higher lipid content compared to those with randomly integrated transgenes. Notably, these transformants showed a 25% increase in DHA content compared to the wild-type strain.

Conclusion This study successfully established a robust homologous recombination system in *Schizochytrium* sp. by identifying a reliable safe harbor site for gene integration. The targeted expression of the KR gene at this site not only enhanced DHA production but also maintained growth and glucose consumption rates, validating the efficacy of the safe-harbor approach. This advancement in synthetic biology and metabolic engineering paves the way for more efficient biotechnological applications in *Schizochytrium* sp.

Keywords *Schizochytrium*, Safe harbor site, 3-ketoacyl-ACP reductase, Docosahexaenoic acid

[†]Ae Jin Ryu and Won-Sub Shin contributed equally to this work.

*Correspondence:
Ji Young Kim
jy.kim2@cj.net
Nam Kyu Kang
nkkang@khu.ac.kr
[1]CJ BIO Research Institute , CJ CheilJedang, Suwon-si, Gyeonggi- do 16495, Republic of Korea
[2]Department of Chemical Engineering, College of Engineering, Kyung Hee University, Yongin 17104, Republic of Korea

Introduction

Thraustochytrids, a group of eukaryotic marine protists, have attracted considerable interest for their role as a rich source of lipid products beneficial for health, which are widely used in the poultry and aquaculture industries, as well as in healthcare settings [1–3]. Particularly, *Thraustochytrids* are known for their impressive ability to synthesize and accumulate various omega-3 fatty acids such as docosahexaenoic acid (DHA, C22:6), eicosapentaenoic acid (EPA, C20:5) and docosapentaenoic acid (DPA, C22:5) [4–6]. Additionally, they produce terpenoids, including carotenoids and squalene [7–10].

Despite the advantages, there remains a critical need for strain development through genetic and metabolic engineering to improve lipid productivity. Although genetic technologies for *Thraustochytrids* are not as advanced as those for bacteria or yeasts, several studies have reported on metabolic engineering to enhance lipid and omega-3 production [11, 12]. To facilitate more sophisticated metabolic engineering, the development of stable heterologous gene expression systems is essential. Due to the position effect, where the specific genomic location of transgene integration can influence its expression, transgene silencing can occur. This effect arises because the integration site may be in genomic regions that are transcriptionally inactive or subject to epigenetic modifications such as DNA methylation and histone modification, which can suppress gene expression [13]. Indeed, the impact of genomic location on gene expression is well-documented across various organisms. For example, in mouse embryonic stem cells, homology-directed repair was found to be more efficient at the NudCD2 locus than at the Hprt locus [14]. Ji et al. (2020) highlighted that integration efficiency in yeast strains lacking non-homologous end joining (NHEJ) varies significantly depending on the target locus [15]. The rate of intrachromosomal homologous recombination in *Salmonella* was also affected by the structure and orientation of chromosomes [16]. While the 18s rDNA region is mainly used as an integration site in *Thraustochytrids* [17–20], more stable and diverse integration sites are required for advanced metabolic engineering.

Thraustochytrids are recognized for their prolific production of polyunsaturated fatty acids (PUFAs). However, the exact mechanisms of their biosynthesis pathways are still under discussion. Typically, two main pathways for lipid biosynthesis are identified: the traditional aerobic fatty acid synthase (FAS) pathway and the anaerobic polyketide synthase (PKS)-like pathway [1, 21]. In the aerobic FAS pathway, synthesis begins with saturated fatty acids (SFAs) such as palmitic (C16) or stearic (C18) acids, which are initially formed through a cyclic chain elongation process. These SFAs are then converted into specific PUFAs via elongation and desaturation steps catalyzed by elongases and desaturases [22]. In contrast, the PKS-like pathway begins by utilizing the SFAs produced in the aerobic process, then further synthesizes long-chain PUFAs through a sequence of enzymatic reactions—condensation, ketoreduction, dehydration, and enoyl reduction—carried out by enzymes such as ketoacyl synthase (KS), ketoacyl reductase (KR), dehydratases (DH), and enoyl reductase (ER) [23].

The PKS pathway efficiently incorporates double bonds into emerging acyl chains, whereas the aerobic pathway integrates double bonds into pre-formed acyl chains. The PKS pathway is relatively more NADPH-efficient, requiring only 14 moles of NADPH to produce one mole of DHA, compared to the FAS pathway, which uses 26 moles of NADPH to produce one mole of DHA [24, 25]. Thus, the PKS pathway is nearly twice as efficient as the FAS pathway in PUFA production. Consequently, *Thraustochytrids* spp., equipped with the PKS system, use less NADPH and produce PUFAs more efficiently than microorganisms without this pathway.

This study aimed to develop genetic engineering tools for the enhanced production of PUFAs in *Schizochytrium* sp. *Schizochytrium*, a notable genus of *Thraustochytrids*, is recognized for its capability to produce substantial amounts of long-chain polyunsaturated fatty acids (LC-PUFAs), particularly DHA [26, 27]. First, a transcriptional hotspot for stable integration and expression of transgenes was identified in *Schizochytrium* sp. A *Schizochytrium* sp. genetic library was constructed by randomly integrating the super folder green fluorescent protein (sfGFP) gene. High-fluorescence mutants were isolated from the library using fluorescence-activated cell sorting (FACS) and characterized to determine the transcriptional hotspot that promotes elevated gene expression in *Schizochytrium* sp. To demonstrate the practical utility of the safe harbor site, the 3-ketoacyl-ACP reductase (KR) gene from the PKS pathway was integrated into this site. It was confirmed that the functional benefits of this hotspot in KR gene expression and enhanced production of PUFAs.

Materials and methods

Strains and culture conditions

In this study, *Schizochytrium sp.* KCTC14661, which is preserved at the Korean Collection for Type Cultures, was utilized. *Schizochytrium* sp. KCTC14661 was maintained in GYPS medium (glucose 26 g/L, peptone 6 g/L, yeast extract 2 g/L, sea salt 12.5 g/L, sucrose 17.1 g/L) or GYPS agar medium containing 1.5% of Bacto agar. Cultivation was conducted in 250 mL baffled flasks with a working volume of 50 mL, maintained at 28 °C. The cultures were agitated at 180 rpm to ensure adequate mixing and aeration.

Plasmid construction

The primers used for this study are summarized in Table S1. Plasmid pUC19-GZG was purchased from addgene (Plasmid #117226). Vector backbone was prepared by PCR using F_GGGS_ShBle and R_GAPDHp-SV40 primers. Codon optimized sfGFP gene was synthesized (Cosmogenetech, South Korea) and amplified using F_SV40_sfGFP and R_sfGFP_GGGS primers to add SV40 sequence (CCCAAGAAGAAGCGCAAGGTG) and GGGS linker sequence (GGCGGAGGTAGC) at 5' and 3' end of the sfGFP gene, respectively. By Gibson assembly, the pUC19-SV40-sfGFP-Shble vector was constructed.

To construct the pUC19-HRsite1-sfGFP-Shble vector, the vector backbone was amplified from the pUC19-SV40-sfGFP-Shble vector using F_Site1_pUC and R_pUC_Site1 primers. The sfGFP-Shble expression cassette was amplified from the pUC19-SV40-sfGFP-Shble vector using F_GAPDHp and R_GAPDHt primers. Using gDNA of *Schizochytrium* sp. KCTC14661 as a template, two primer sets (F_pUC_Site1 and R_Site1_GAPDHp, F_GAPDHt_Site1 and R_Site1_pUC) were used to amplify homology arms. The amplicons were ligated by Gibson assembly.

To construct the pUC19-HRsite2-sfGFP-Shble vector, the vector backbone was amplified from the pUC19-SV40-sfGFP-Shble vector using F_Site2_pUC and R_pUC_Site2 primers. Using gDNA of *Schizochytrium* sp. KCTC14661 as a template, two primer sets (F_pUC_Site2 and R_Site2_GAPDHp, F_GAPDHt_Site2 and R_Site2_pUC) were used to amplify homology arms. Altogether with the sfGFP-Shble expression cassette which was used in pUC19-HRsite1-sfGFP-Shble vector construction, amplicons were ligated by Gibson assembly.

To construct the pUC19-HRsite2-KR-Shble vector, the vector backbone was amplified from the pUC19-HRsite2-sfGFP-Shble vector using F_HSP70t_GAPDHp and R_Site2_bTUBp primers. Using gDNA of *Schizochytrium* sp. KCTC14661 as template, *KR* (3-ketoacyl-ACP reductase) gene (F_bTUBp_KR and R_KR_HSP70t primers), 5' region (1582 bp) of beta-tubulin gene (F_Site2_bTUBp and R_bTUBp_KR primers) and 3' region (476 bp) of HSP70 gene (F_KR_HSP70t, R_HSP70t_GAPDHp primers) were amplified (Table S1). Then, the amplicons were ligated by Gibson assembly.

Transformation of Schizochytrium sp.

In a 250 mL flask, 50 mL of GYPS medium (Glucose 26 g/L, Peptone 6 g/L, Yeast extract 2 g/L, Sea salt 12.5 g/L, Sucrose 17.1 g/L) was added, and *Schizochytrium* sp. were incubated at 28℃ for 48 h. The cultured cells were transferred to two EP tubes containing 1 mL and centrifuged for 1 min. After removing the supernatant from the centrifuged microalgal culture, the concentrated microalgal cells were resuspended in 1X BSS solution (10 mM KCl, 10 mM NaCl, and 3 mM $CaCl_2$) and then centrifuged. The supernatant was removed, and the microalgal cells were resuspended in 50 mM sucrose, followed by centrifugation. This process was repeated three times. Subsequently, 0.1 mL of 50 mM sucrose was added to the concentrated microalgal, and the samples were transformed using electroporation. The cell suspension was mixed with 1 μg of cassette, which was amplified with proper primer sets: F_GAPDHp and R_GAPDHt for insertional mutagenesis; F_HR1_cassette and R_HR1_cassette for homologous recombination targeting the HRSite 1 locus; F_HR2_cassette and R_HR2_cassette for homologous recombination targeting the HRSite 2 locus (Table S1). The mixture was added to 2 mm gap cuvette (Bio-rad, USA), and then electroporation was conducted (2500 V cm^{-1} field strength, 50 μF capacitance, 500 Ω) using Gene Pulser (Bio-rad, USA). The cells were resuspended in 1 mL of GYPS medium and then incubated at 28℃ for 1 h. The recovered cells were plated onto GYPS agar medium containing 15 μg mL^{-1} zeocin. Survived colonies were transferred to new agar plates containing zeocin and maintained for further use.

Fluorescence-activated cell sorting analysis

Schizochytrium sp. was inoculated into GYPS medium and incubated at 28℃ for 24 h. Each sample was analyzed using BD Accuri™ C6 Plus Flow Cytometer (BD Bioscience, USA). Fluorescence was detected using an excitation laser of 488 nm and 530–533 nm FL1 channel filter. Mean fluorescence intensity was calculated based on fluorescence intensities of 10,000 cells.

PCR analysis of mutants

Genomic DNA was extracted using FastDNA™ SPIN Kit for Soil (MP Biomedicals, USA). Extracted genomic DNA samples were used as templates for PCR. Homologous recombination of sfGFP-Shble expression cassette into HRsite 1 was confirmed with F_site1_HR_C_100 and R_GAPDHp_400 primers. For site 2, F_Site2_HR_C_100 and R_GAPDHp_400 primers were used. *Sh*ble gene fragment was amplified with F_cj_BleoR and R_cj_BleoR primers. Homologous recombination of *KR* expression cassette was confirmed with F_HR site2_C and R_HR site2_C_rev primers. (Table S1)

Inverse PCR analysis

Genomic DNA samples of wild-type *Schizochytrium* sp. KCTC14661 and transformants were subjected to restriction enzyme treatment (HindIII, NEB). T4 ligase (NEB) was then added to each sample and incubated overnight. The ligate samples were used to verify the chromosomal insertion site. First, the ligate was subjected to PCR as a template with F_Shble_2700 and R_sfGFP_1800 primers. The product of the first PCR was then used as a

template for the second PCR with F_Shble_2800 and R_SV40_1740 primers (Table S1). The amplicons in the final PCR product were separated by electrophoresis and purified to analyze its sequence. With the sequencing results, a BLAST search was conducted to verify the insertion site in the transformants.

Fatty acid methyl ester analysis

The FAME analysis was performed as previously described [28]. 50 mL of cell cultures were collected through centrifugation at 4,000 rpm for 15 min (Supra-22 k, Hanil Science Industrial, Republic of Korea). The samples were then washed with deionized water and lyophilized for 3 days (FD5508, ilShin BioBase, Republic of Korea). Lipids were extracted from the dried biomass using a modified version of Folch's method [29]. A mixture of chloroform and methanol (2:1, v/v) was added to the biomass and thoroughly mixed for 10 min. Heptadecanoic acid (C11:0) was added at 0.5 mg as an internal standard. The mixture was then treated with 1 mL of methanol and 300 µL of sulfuric acid and heated to 100 °C for 20 min for transesterification. The resulting FAMEs were analyzed using a gas chromatograph equipped with a flame-ionized detector (HP 6890; Agilent Technologies, CA, USA) and an HP-INNOWax polyethylene glycol column (HP 19091 N-213; Agilent, CA, USA). Quantification of FAMEs was based on comparisons with a 37-component FAME standard mix (F.A.M.E. MIX C8-C24; Sigma-Aldrich, MO, USA).

Results and discussion

Identification and characterization of transgene integration sites in Schizochytrium sp. KCTC14661

To identify a safe harbor site for gene expression in *Schizochytrium* sp. KCTC14661, a random insertional mutagenesis was conducted by employing the plasmid pUC19-SV40-sfGFP-Shble [30]. The GFP-Shble expression cassette within this plasmid was amplified by PCR using primers F_GAPDHp and R_GAPDHt, and subsequently introduced into *Schizochytrium* sp. (Fig. 1a). Transformants were selected on a Zeocin-containing selective agar medium, and their GFP expression levels were analyzed using fluorescence-activated cell sorting (FACS). Notably, transformants 23 and 42 showed high levels of GFP expression, and green fluorescence was shown under a fluorescence microscope (Fig. 1b and c). To determine the integration sites of these transformants, inverse PCR was conducted, followed by sequencing of the PCR products (Fig. 1d). BLASTX analysis of these sequences revealed that the GFP expression cassettes in transformants 23 and 42 were integrated at 3 kb downstream region of agmatine deiminase gene and 3.2 kb upstream region of the cytochrome c, respectively, designated as HRsite 1 and HRsite 2 (Table S2 and S3).

Agmatine deiminase is crucial in the agmatine catabolism pathway, catalyzing the conversion of agmatine into N-carbamoylputrescine and ammonia [31]. This enzyme is vital for microbial metabolism, allowing the utilization of agmatine as a nitrogen source. It also influences polyamine biosynthesis, which is essential for diverse physiological roles in stress response, growth regulation, and cell signaling. Previous research highlighted that the metabolism of agmatine to putrescine enhances bacterial growth [32]. Cytochrome c is a small heme protein found universally in the mitochondria of eukaryotes and many aerobic bacteria, playing a pivotal role in the electron transport chain. This protein mediates electron transfer between Complex III (cytochrome bc1 complex) and Complex IV (cytochrome c oxidase) in the mitochondrial membrane, essential for cellular respiration and energy production [33]. While agmatine deiminase and cytochrome c in *Schizochytrium* have not been well studied, they may play significant roles in cell growth with stable and constitutive expression. Thus, the high GFP expression observed in the transformants 23 and 42 suggests that HRsites 1 and 2, located near the agmatine deiminase and cytochrome c loci, facilitate stable transgene integration and robust gene expression in *Schizochytrium*.

Efficiency of homologous recombination at designated safe harbor sites

Targeted transformations were carried out at HRsite 1 and HRsite 2 using homologous recombination. The transformation was conducted using sfGFP and *Sh*ble expression cassettes flanked by 1 kb of homologous regions on each side (Fig. 2a). Several transformants were generated and subjected to colony PCR to verify the integration of the transgene at the targeted sites. The colony PCR results showed successful integration at HRsite 1 and 2 for multiple transformants (Fig. 2b). Specifically, out of 30 transformants analyzed for each site, only two showed integration at HRsite 1. In comparison, integration at HRsite 2 was confirmed in 11 transformants. The rest of the transformants had the transgene integrated at random locations.

FACS analysis revealed that the transformants targeted at HRsite 1 and 2 exhibited an average relative green fluorescence intensity of 714.61 and 841.54, respectively. Compared to the wild-type (WT) fluorescence intensity of about 319.21, the targeted transformants showed significantly enhanced transgene expression. Particularly, as HRsite 2 was more efficient for integration and gene expression than HRsite 1, further studies focused on HR site 2.

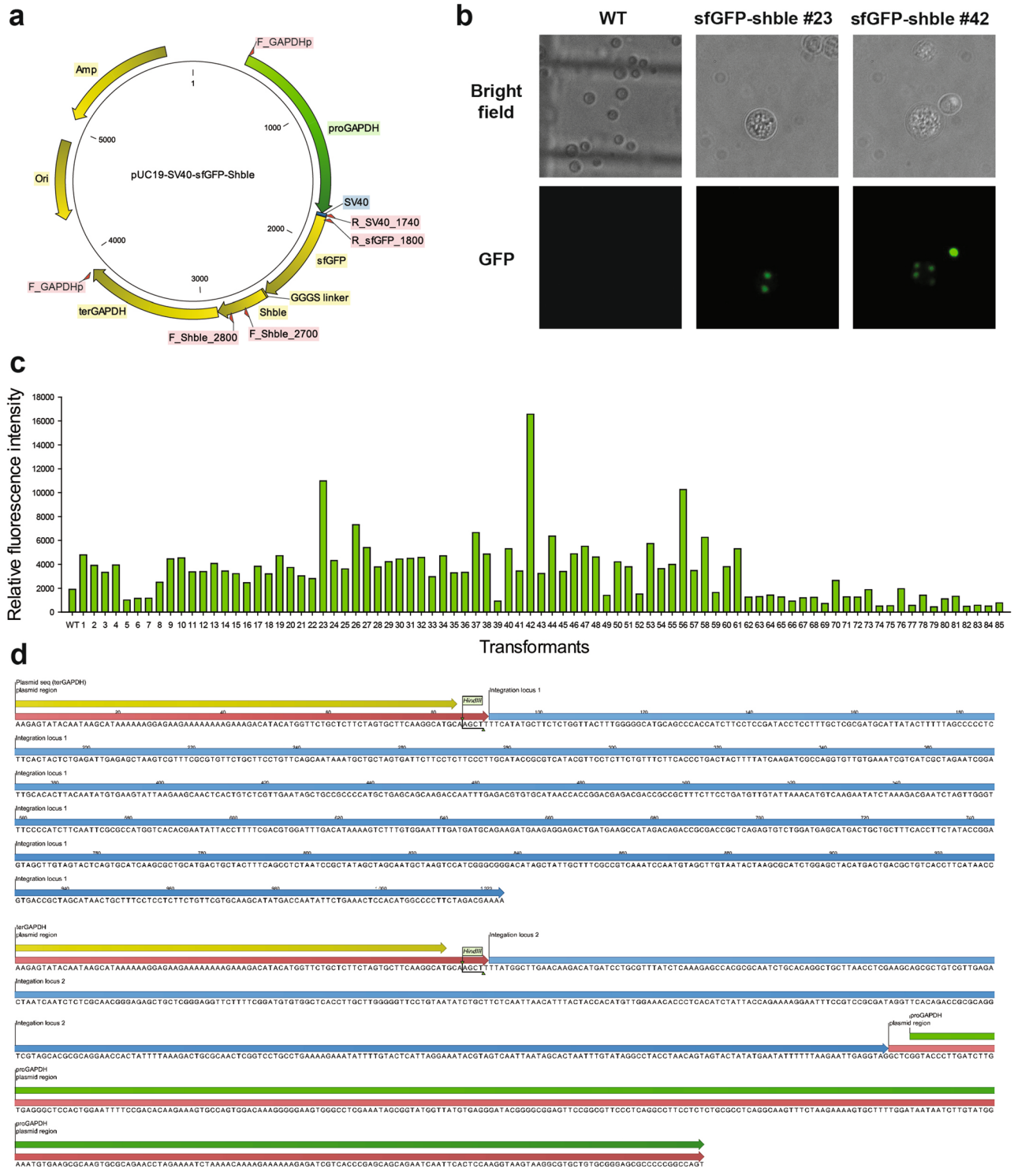

Fig. 1 Identification of transcriptional hotspots through insertional mutagenesis and FACS-based screening. **a** The pUC19-SV40-sfGFP-Shble plasmid. **b** Fluorescence microscopy image comparing *Schizochytrium* sp. KCTC14661 WT and sfGFP-expressing transformant. **c** Analysis of relative fluorescence intensity of sfGFP-expressing transformants by FACS. **d** Sequence analysis of the integration site via inverse PCR

Analysis of 3-ketoacyl-ACP reductase gene integration at HRsite 2

The pUC19-HRsite2-KR-Shble vector was constructed to integrate the KR of polyketide synthase, involved in the biosynthesis of PUFAs, into HRsite 2 by adding left and right homologous flanking regions, each 1,000 bp in length (Fig. 3a). The KR enzyme is essential in PKS for reducing 3-ketoacyl-ACP to 3-hydroxyacyl-ACP, a

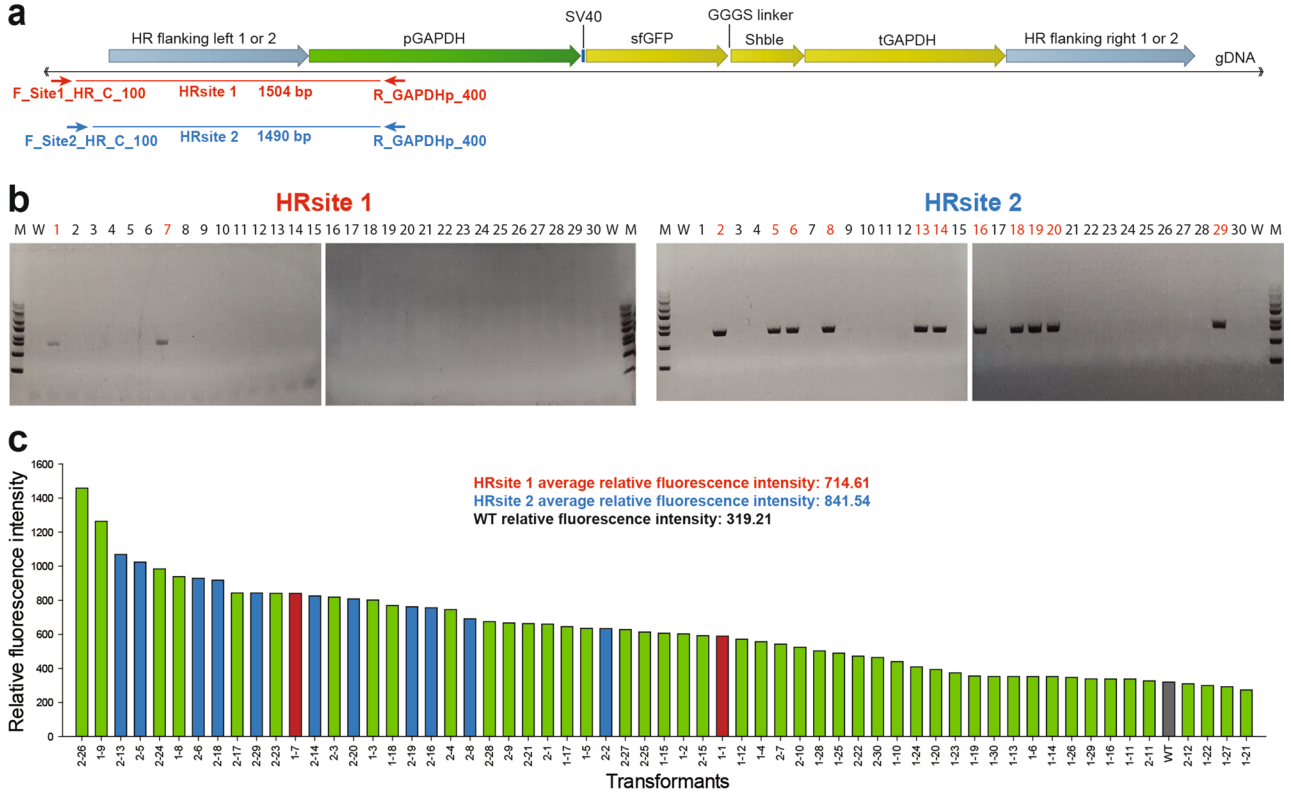

Fig. 2 Targeted homologous recombination at HRsite 1 and 2. **a** Schematic representation of the integration of linearized pUC19-SV40-sfGFP-Shble into HRsite 1 and 2, including confirmation primers. **b** Genomic DNA PCR results confirming homologous recombination. **c** Relative fluorescence measured by FACS in sfGFP-expressing transformants resulting from targeted recombination. Red and blue bars indicate successful homologous recombination at HRsite 1 and HRsite 2, respectively. Green bars represent transformants with random integration

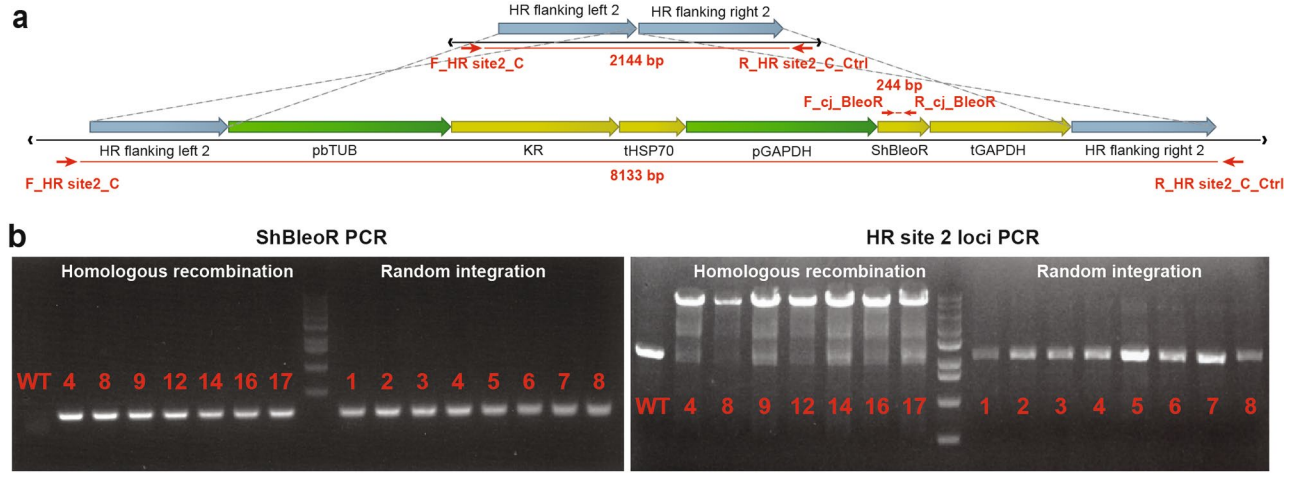

Fig. 3 Integration of the pUC19-HRsite2-KR-Shble vector into HRsite 2. **a** Schematic diagram showing the integration of linearized pUC19-SV40-sfGFP-Shble into HRsite 2 with confirmation primers. **b** Genomic DNA PCR results confirming homologous recombination

critical step in elongating fatty acid chains [34]. This integration into HRsite 2 aimed to explore the stable expression of genes and their associated stable phenotypes. Additionally, random integration using the KR expression cassette without homologous recombination flanking regions was conducted to compare the efficiency of homologous recombination at HRsite 2. After transformation, colony PCR was conducted to examine if the transgene was integrated into the targeted site (Fig. 3b). The F_cj_BeloR and R_cj_BleoR primers were used to confirm the *Sh*ble marker gene, which could be detected in both homologous recombination and random

integration transformations. Another colony PCR using F_HR site2_C and R_HR site2_C_ctrl was conducted to investigate the transgene integration into HRsite 2 (Table S1). In cases of homologous recombination where the transgene was integrated into the HRsite 2, the band size was 8,133 bp. Conversely, in random integration mutagenesis, where the transgene was integrated at random sites, the PCR band size of HRsite 2 was only 2,144 bp, the same as that of the wild type (WT). Among 20 transformants selected from the homologous recombination transformation, the transgene was integrated into the targeted sites in 7 transformants, thus yielding an integration efficiency of approximately 35%.

Comparative phenotypic analysis of homologous recombination and random integration transformants

Phenotypic comparisons were conducted between 7 homologous recombination (KR-HR) transformants and 8 random integration (KR-RI) transformants of the KR overexpression in *Schizochytrium* sp. KCTC14661 (Fig. S1-4). When analyzing growth via optical density at 562 nm (OD_{562nm}), the KR-HR transformants achieved an average OD_{562nm} of approximately 47 at 46 h, which was markedly higher than the 36 observed in the KR-RI transformants (Fig. 4a, S1). Notably, the deviation of growth measurements among the KR-HR transformants was significantly lower than that observed in the KR-RI group, indicating a more consistent growth pattern in the KR-HR transformants.

Regarding glucose consumption, all KR-HR transformants utilized the total provided concentration of 26 g/L glucose in 46 h. In contrast, only three of the KR-RI transformants were able to completely consume the available glucose (Fig. 4b, S2). This pattern of glucose consumption highlights the greater consistency and efficiency among the KR-HR transformants, evidenced by a more rapid decrease in glucose levels and less deviation as compared to the KR-RI transformants.

Fatty acid methyl ester (FAME) content analysis showed that the KR-HR transformants had an average FAME content of 45% with a deviation of only 1.4%, suggesting consistent lipid production. In terms of the KR-RI transformants, FAME analysis was conducted on only six samples because strains KR-RI #2 and #8 exhibited lower glucose consumption and insufficient growth, which did not support lipid analysis (Fig. S2 and S3). These 6 KR-RI transformants showed a similar average FAME content of about 45% as compared to the KR-HR transformants. However, the deviation was markedly higher at 6.3%, indicating a greater inconsistency in lipid production (Fig. 4c, S3). The inability of transformants #2 and #8 to grow adequately suggests that transgene expression via random integration was considerably unstable compared to homologous recombination at HRsite 2.

The fatty acid composition analysis (Fig. 4d) further supports these findings. Both groups showed similar profiles for palmitic acid (PA, C16:0), docosahexaenoic acid (DHA, C22:6), docosapentaenoic acid (DPA, C22:5), and eicosapentaenoic acid (EPA, C20:5). However, the HR transformants exhibited a slightly higher average content of DHA. The deviation of PA and DHA contents was greater in the RI transformants than in the HR group. This indicates enhanced overall stability and improved specific fatty acid production in HR-based KR overexpressing transformants.

These results demonstrated that the integration of transgenes into HRsite 2, the safe harbor site, significantly enhanced phenotypic consistency and the efficiency of metabolic gene expression in *Schizochytrium* sp. KCTC14661. The differences in phenotype stability and metabolic efficiency between the HR and RI transformants clearly showed the advantages of targeted genetic integration for biotechnology applications.

Enhanced DHA production through targeted KR gene integration in Schizochytrium sp.

Among the homologous recombination transformants, KR-HR16 was chosen for comparison with the *Schizochytrium* sp. KCTC14661 WT (Fig. S1-4). The KR-HR16 strain exhibited not only better growth but also a slightly faster rate of glucose consumption than WT (Fig. 5a and b). Furthermore, FAME content in KR-HR16 was 46%, which was higher than 43% observed in WT (Fig. 5c). Notably, KR-HR16 showed a decrease in PA content and an increase in DHA content. Specifically, the PA and DHA contents in KR-HR16 were 28% and 50%, respectively, whereas they were 36% and 40% in WT, respectively. Likewise, the negative effect of the transgene integration into HRsite 2 on growth, glucose consumption, and lipid production was not observed. As this integration into HRsite 2 does not disrupt the coding sequence of cytochrome c, which is crucial for cell growth, the expression of KR in HRsite 2 appears to have no detrimental effects on growth or lipid production.

The role of KR in the PKS pathway involves catalyzing the reduction of 3-ketoacyl-ACP to 3-hydroxyacyl-ACP. Previous research has demonstrated that integrating KR and dehydratase genes into the 18s rDNA region significantly increased total fatty acid and DHA content in *Aurantiochytrium limacinum* [18]. Moreover, heterologous overexpression of *Schizochytrium* KR in *Yarrowia lipolytica* led to a decrease in PA levels and a 1.13-fold increase in polyunsaturated fatty acids (PUFAs), particularly EPA, compared to the control strain [35]. These findings align with our results, where KR-HR16 displayed reduced PA levels and enhanced PUFA content. Notably, in *Schizochytrium*, there was a specific increase in DHA production, consistent with the tendency of

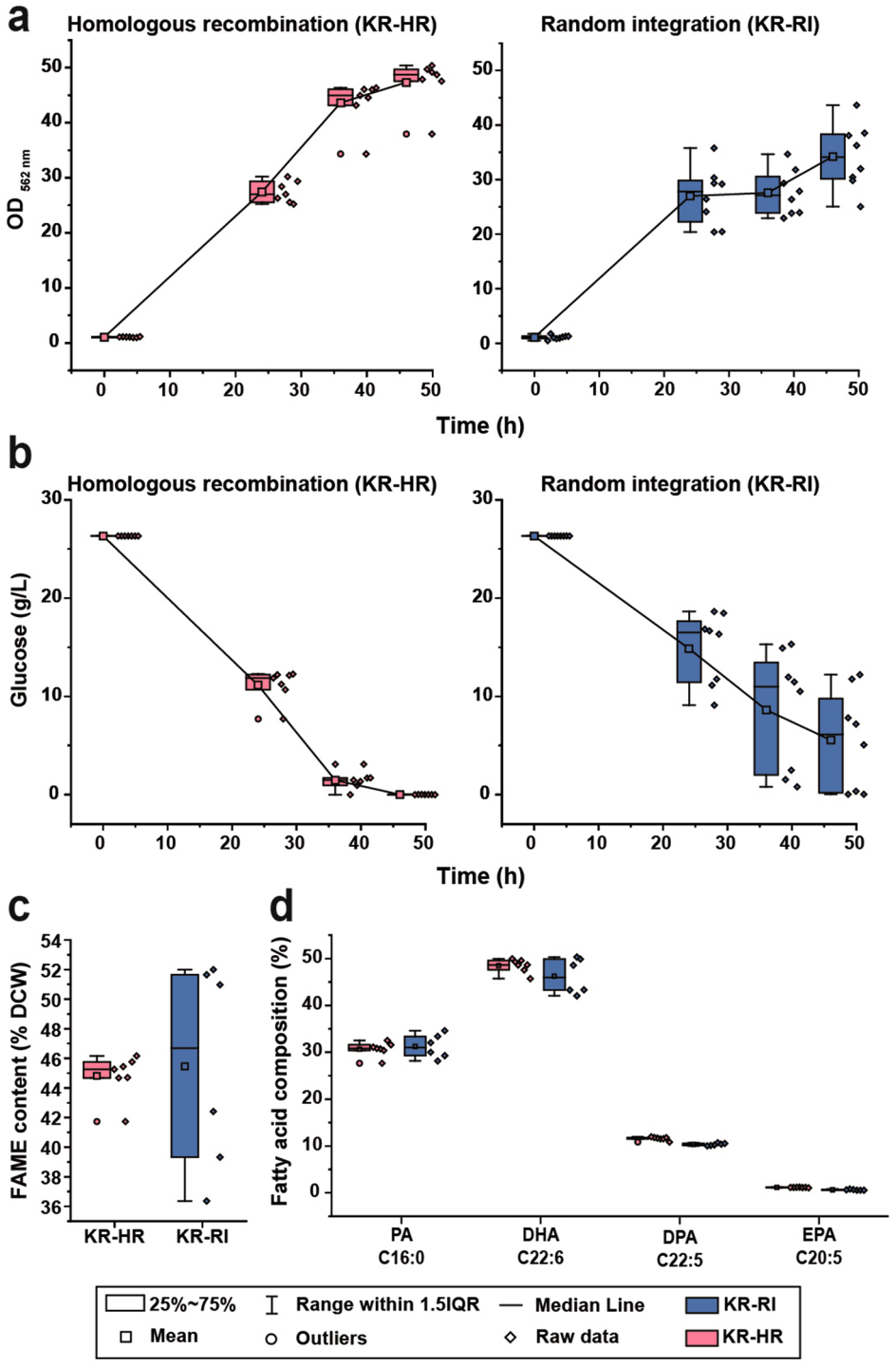

Fig. 4 Phenotypic assays of KR-overexpressing transformants. Phenotypic comparisons were conducted between 7 homologous recombination transformants at HRsite 2 (KR-HR) and 8 randomly integrated transformants (KR-RI) in *Schizochytrium sp.* KCTC14661. **a** Growth curves with box-and-whisker plots. **b** Glucose consumption profiles with box-and-whisker plots. **c** Fatty acid methyl ester (FAME) contents shown using box-and-whisker plots. **d** Profiles of fatty acid compositions displayed using box-and-whisker plots. Each set of 7 KR-HR and 8 KR-RI transformants was cultured in duplicate, and data for KR-HR and KR-RI were averaged. Additional details on the cultivation data of each strain are presented in the Fig. S1-4. Cultivation was carried out in 250 mL baffled flasks containing 50 mL of GYPS medium, maintained at 28 °C, and agitated at 180 rpm. FAME and fatty acid compositions were analyzed at 46 h

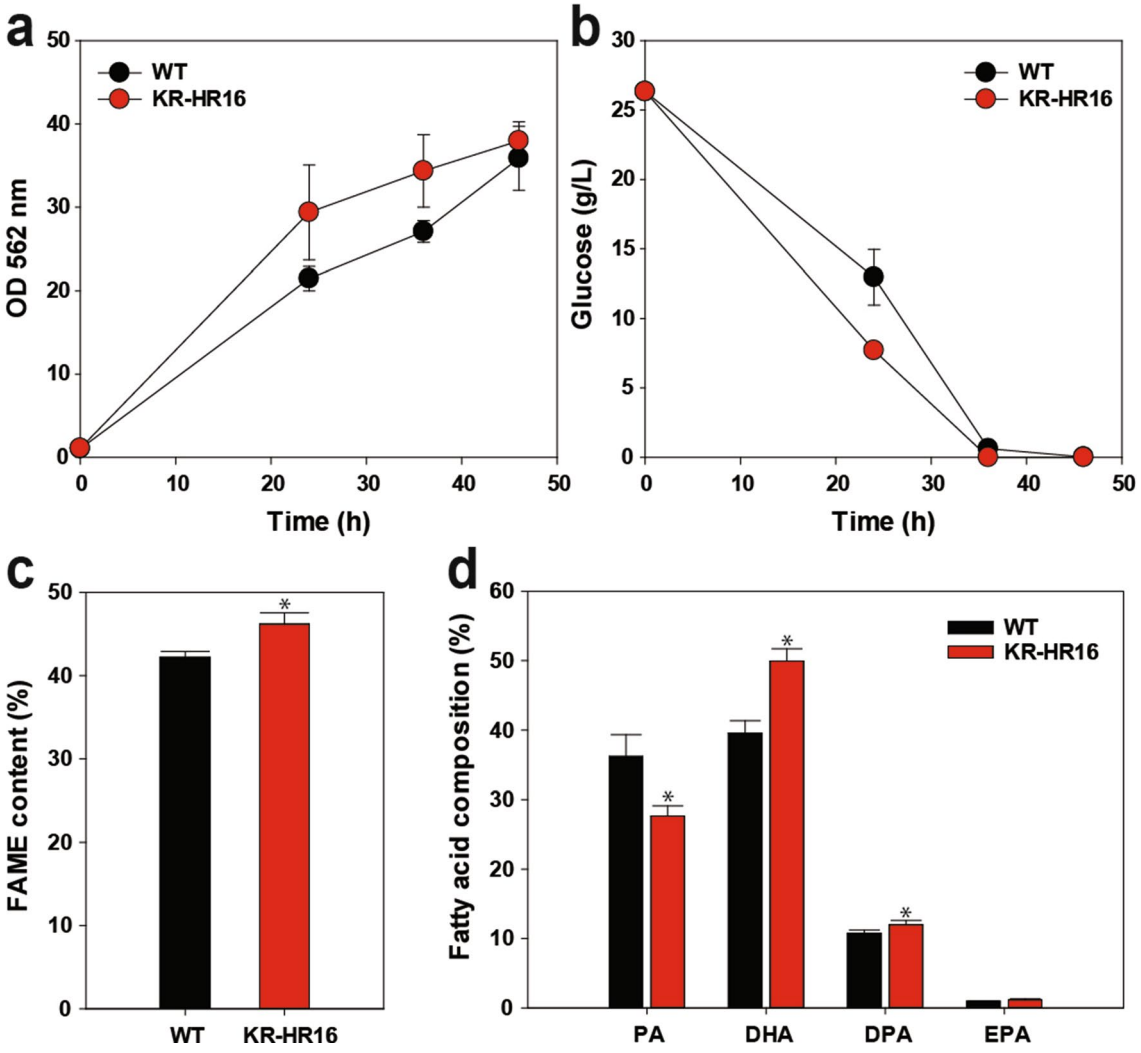

Fig. 5 Comparison of KR overexpression transformants with WT. **a** Growth curves measured by optical density at 562 nm. **b** Glucose consumption profiles. **c** FAME contents. **d** Profiles of fatty acid compositions. Cultivation was performed in 250 mL baffled flasks with 50 mL of GYPS medium at 28 °C, agitated at 180 rpm. FAME and fatty acid compositions were analyzed at 46 h. The data points represent the average of samples and error bars indicate standard deviation ($n=3$). Significant differences compared with WT, as indicated by asterisks (*$p<0.05$, **$p<0.01$, ***$p<0.001$), were determined by Student's t-test

Schizochytrium to accumulate more DHA than EPA. In addition, compared to other studies on DHA production in *Schizochytrium* (Table S4), the DHA content in our study based on total fatty acids (50%) was higher. When assessing DHA content relative to biomass, our results were superior to all other studies except those involving engineered strains overexpressing ATP-citrate lyase and acetyl-CoA carboxylase [36]. This discrepancy may be attributed to differences in culture conditions. Therefore, KR overexpression presents a promising strategy for enhancing DHA production in *Schizochytrium*.

The influence of chromosomal positioning on gene expression, known as the chromosome position effect, is a pivotal consideration in metabolic engineering [37]. Key factors affecting gene expression at different chromosomal locations include the degree of DNA compaction, proximity to DNA replication initiation sites, and the availability of regulatory factors. Studies using reporter genes in various microbes, such as *E. coli*, *Bacillus subtilis*, and *S. cerevisiae*, have clearly demonstrated that gene expression levels can significantly vary depending on the site of integration due to chromosome position effects [38–40]. This underscores the crucial role of chromosomal location in influencing gene activity. Given that gene manipulation and metabolic engineering in microalgae is challenging, recognizing position effects in these organisms is essential. Garmendia et al. (2021) showed that chromosomal location determines intrachromosomal homologous recombination [16]. This study also suggested that orientation of gene in bacterial chromosome affects recombination rate. In our study, site 1 and site 2 were located within the same contig, but

the distance between the two sites exceeded 800,000 bp. The disparate locations of these sites likely influenced their accessibility to the transgene expression cassette. However, we could not find a similar study or discussion in *Schizochytrium*. Another study in *Nannochloropsis salina*, photosynthetic microalgae, has explored the impacts of position effects [30]. This study has led to the identification of safe harbor sites and the development of stable transgene expression systems using CRISPR/Cas9 technology. It is anticipated that similar advanced metabolic engineering was achieved in *Schizochytrium*, heterotrophic microalgae, based on the safe-harboring transcription hotspot identified in this study.

Synthetic biology and its tools are essential for advanced metabolic engineering, with stable gene integration and expression being fundamental [37]. In this study, we developed valuable tools and strategies applicable to the synthetic biology of *Schizochytrium* by delving into chromosomal position effects and gene integration methods. These advances have enhanced our understanding of gene expression modulation and improved our capacity to engineer *Schizochytrium* for the efficient production of lipid-derived bioproducts. Integrating these synthetic biology approaches with metabolic engineering sets the stage for future innovative biotechnological advancements and sustainable industrial applications using *Schizochytrium*.

Conclusion

This study established an effective homologous recombination system in *Schizochytrium* sp. KCTC14661 by identifying a safe harbor site, notably HRsite 2 associated with cytochrome c. Transgene expression in HRsite 2 exhibited enhanced sfGFP expression and higher efficiency in homologous recombination. Targeting HRsite 2 for expressing the KR gene, which is crucial in the PKS pathway, resulted in consistent phenotypes and increased DHA production without a deficiency in growth and glucose consumption. This validates the safe-harboring approach, advancing synthetic biology and metabolic engineering in *Schizochytrium* sp.

Abbreviations

KR 3	ketoacyl-ACP reductase
DHA	Docosahexaenoic acid
EPA	Eicosapentaenoic acid
DPA	Docosapentaenoic acid
PUFAs	Polyunsaturated fatty acids
FAS	Fatty acid synthase
PKS	Polyketide synthase
SFAs	Saturated fatty acids
KS	Ketoacyl synthase
KR	Ketoacyl reductase
DH	Dehydratases
ER	Enoyl reductase
sfGFP	Super folder green fluorescent protein
FACS	Fluorescence-activated cell sorting
FAME	Fatty acid methyl ester

Supplementary Information

The online version contains supplementary material available at https://doi.org/10.1186/s13036-024-00447-y.

Supplementary Material 1

Acknowledgements

Not Applicable.

Author contributions

A. J. R. and W.-S. S. contributed to the conceptualization, data curation, methodology, formal analysis, investigation, writing of the original draft, and visualization. S. J., Y. L., Y. P., and Y. C. contributed to the methodology, formal analysis, and investigation. J. Y. K. and N. K. K. contributed to the conceptualization, writing of the review and editing, supervision, and funding acquisition.

Funding

This work was supported by a grant from Kyung Hee University in 2024 (KHU- 20241099).

Data availability

No datasets were generated or analysed during the current study.

Declarations

Ethics approval and consent to participate

Not applicable.

Consent for publication

Not applicable.

Competing interests

The authors declare no competing interests.

Received: 8 August 2024 / Accepted: 11 September 2024
Published online: 10 October 2024

References

1. Du F, Wang YZ, Xu YS, Shi TQ, Liu WZ, Sun XM, et al. Biotechnological production of lipid and terpenoid from thraustochytrids. Biotechnol Adv. 2021;48:107725. https://doi.org/10.1016/j.biotechadv.2021.107725.
2. Sohedein MNA, Wan-Mohtar WAI, Ilham Z, Babadi AA, Yeong HY, Phang SM. Vital parameters for biomass, lipid, and carotenoid production of thraustochytrids. J Appl Phycol. 2020;32:1003–16. https://doi.org/10.1007/s10811-019-01970-y.
3. Fan KW, Chen F. Production of high-value products by Marine Microalgae Thraustochytrids. Bioprocessing for value-added products from renewable resources. Amsterdam: Elsevier; 2007. pp. 293–323. S.-T. Yang, Editor.
4. Raghukumar S. Thraustochytrid Marine protists: production of PUFAs and other Emerging technologies. Mar Biotechnol (NY). 2008;10:631–40. https://doi.org/10.1007/s10126-008-9135-4.
5. Chang KJ, Mansour MP, Dunstan GA, Blackburn SI, Koutoulis A, Nichols PD. Odd-chain polyunsaturated fatty acids in thraustochytrids. Phytochemistry. 2011;72:1460–5. https://doi.org/10.1016/j.phytochem.2011.04.001.
6. Patel A, Mahboubi A, Horvath IS, Taherzadeh MJ, Rova U, Christakopoulos P, et al. Volatile fatty acids (VFAs) generated by anaerobic digestion serve as feedstock for Freshwater and Marine Oleaginous microorganisms to produce Biodiesel and added-value compounds. Front Microbiol. 2021;12:614612. https://doi.org/10.3389/fmicb.2021.614612.
7. Aki T, Hachida K, Yoshinaga M, Katai Y, Yamasaki T, Kawamoto S, et al. Thraustochytrid as a potential source of carotenoids. J Am Oil Chem Soc. 2003;80:789–94. https://doi.org/10.1007/s11746-003-0773-2.
8. Armenta RE, Burja A, Radianingtyas H, Barrow CJ. Critical assessment of various techniques for the extraction of carotenoids and co-enzyme Q10 from the Thraustochytrid strain ONC-T18. J Agric Food Chem. 2006;54:9752–8. https://doi.org/10.1021/jf061260o.

9. Jiang Y, Fan KW, Wong RT, Chen F. Fatty acid composition and squalene content of the marine microalga Schizochytrium mangrovei. J Agric Food Chem. 2004;52:1196–200. https://doi.org/10.1021/jf035004c.
10. Patel A, Liefeldt S, Rova U, Christakopoulos P, Matsakas L. Co-production of DHA and squalene by thraustochytrid from forest biomass. Sci Rep. 2020;10. https://doi.org/10.1038/s41598-020-58728-7.
11. Jesionowska M, Ovadia J, Hockemeyer K, Clews AC, Xu Y. EPA and DHA in microalgae: Health benefits, biosynthesis, and metabolic engineering advances. Journal of the American Oil Chemists Society 2023;100:831-842.10.1002/aocs.12718.
12. Han X, Liu Y, Yuan Y, Chen Z. Metabolic engineering of Schizochytrium sp. for superior docosahexaenoic acid production. Algal Res. 2024;77:103355. https://doi.org/10.1016/j.algal.2023.103355.
13. Singh J, Freeling M, Lisch D. A position effect on the heritability of epigenetic silencing. PLoS Genet. 2008;4:e1000216. https://doi.org/10.1371/journal.pgen.1000216.
14. Hirotsune S, Kiyonari H, Jin M, Kumamoto K, Yoshida K, Shinohara M et al.,: *Enhanced homologous recombination by the modulation of targeting vector ends. Scientific Reports 2020;10:2518.10.1038/s41598-020-58893-9*
15. Ji Q, Mai J, Ding Y, Wei Y, Ledesma-Amaro R, Ji X-J. Improving the homologous recombination efficiency of Yarrowia Lipolytica by grafting heterologous component from Saccharomyces cerevisiae. Metabolic Eng Commun. 2020;11:e00152. https://doi.org/10.1016/j.mec.2020.e00152.
16. Garmendia E, Brandis G, Guy L, Cao S, Hughes D. Chromosomal location determines the rate of Intrachromosomal homologous recombination in Salmonella. mBio. 2021;12. https://doi.org/10.1128/mbio.01151-01121.10.1128/mbio.01151-21.
17. Wang F, Bi Y, Diao J, Lv M, Cui J, Chen L, et al. Metabolic engineering to enhance biosynthesis of both docosahexaenoic acid and odd-chain fatty acids in Schizochytrium sp. S31. Biotechnol Biofuels. 2019;12:141. https://doi.org/10.1186/s13068-019-1484-x.
18. Liu Z, Zang X, Cao X, Wang Z, Liu C, Sun D, et al. Cloning of the pks3 gene of Aurantiochytrium Limacinum and functional study of the 3-ketoacyl-ACP reductase and dehydratase enzyme domains. PLoS ONE. 2018;13:e0208853. https://doi.org/10.1371/journal.pone.0208853.
19. Yan J, Cheng R, Lin X, You S, Li K, Rong H, et al. Overexpression of acetyl-CoA synthetase increased the biomass and fatty acid proportion in microalga Schizochytrium. Appl Microbiol Biotechnol. 2013;97:1933–9. https://doi.org/10.1007/s00253-012-4481-6.
20. Sakaguchi K, Matsuda T, Kobayashi T, Ohara J, Hamaguchi R, Abe E, et al. Versatile transformation system that is applicable to both multiple transgene expression and gene targeting for Thraustochytrids. Appl Environ Microbiol. 2012;78:3193–202. https://doi.org/10.1128/AEM.07129-11.
21. Chi G, Xu Y, Cao X, Li Z, Cao M, Chisti Y, etal, et al. Production of polyunsaturated fatty acids by Schizochytrium (Aurantiochytrium) spp. Biotechnol Adv. 2022;55:107897. https://doi.org/10.1016/j.biotechadv.2021.107897.
22. Ratledge C. Fatty acid biosynthesis in microorganisms being used for single cell oil production. Biochimie. 2004;86:807–15. https://doi.org/10.1016/j.biochi.2004.09.017.
23. Meesapyodsuk D, Qiu X. Biosynthetic mechanism of very long chain polyunsaturated fatty acids in Thraustochytrium sp. 26185. J Lipid Res. 2016;57:1854–64. https://doi.org/10.1194/jlr.M070136.
24. Ratledge C. The role of malic enzyme as the provider of NADPH in oleaginous microorganisms: a reappraisal and unsolved problems. Biotechnol Lett. 2014;36:1557–68. https://doi.org/10.1007/s10529-014-1532-3.
25. Gemperlein K, Dietrich D, Kohlstedt M, Zipf G, Bernauer HS, Wittmann C, et al. Polyunsaturated fatty acid production by Yarrowia Lipolytica employing designed myxobacterial PUFA synthases. Nat Commun. 2019;10:4055. https://doi.org/10.1038/s41467-019-12025-8.
26. Morabito C, Bournaud C, Maes C, Schuler M, Aiese Cigliano R, Dellero Y, et al. The lipid metabolism in thraustochytrids. Prog Lipid Res. 2019;76:101007. https://doi.org/10.1016/j.plipres.2019.101007.
27. Bao Z, Zhu Y, Feng Y, Zhang K, Zhang M, Wang Z et al.,: *Enhancement of lipid accumulation and docosahexaenoic acid synthesis in Schizochytrium sp. H016 by exogenous supplementation of sesamol. Bioresour Technol 2022;345:126527.10.1016/j.biortech.2021.126527*
28. Kang NK, Kim EK, Kim YU, Lee B, Jeong WJ, Jeong BR, et al. Increased lipid production by heterologous expression of AtWRI1 transcription factor in Nannochloropsis salina. Biotechnol Biofuels. 2017;10:231. https://doi.org/10.1186/s13068-017-0919-5.
29. Folch J, Lees M, Sloane Stanley GH. A simple method for the isolation and purification of total lipides from animal tissues. J Biol Chem. 1957;226:497–509.
30. Ryu AJ, Jeong BR, Kang NK, Jeon S, Sohn MG, Yun HJ, et al. Safe-harboring based novel genetic toolkit for Nannochloropsis salina CCMP1776: efficient overexpression of transgene via CRISPR/Cas9-Mediated knock-in at the transcriptional hotspot. Bioresour Technol. 2021;340:125676. https://doi.org/10.1016/j.biortech.2021.125676.
31. Jones JE, Dreyton CJ, Flick H, Causey CP, Thompson PR. Mechanistic studies of agmatine deiminase from multiple bacterial species. Biochemistry. 2010;49:9413–23. https://doi.org/10.1021/bi101405y.
32. del Rio B, Linares DM, Ladero V, Redruello B, Fernandez M, Martin MC, et al. Putrescine production via the agmatine deiminase pathway increases the growth of Lactococcus lactis and causes the alkalinization of the culture medium. Appl Microbiol Biotechnol. 2015;99:897–905. https://doi.org/10.1007/s00253-014-6130-8.
33. Srinivasan S, Avadhani NG. Cytochrome c oxidase dysfunction in oxidative stress. Free Radic Biol Med. 2012;53:1252–63. https://doi.org/10.1016/j.freeradbiomed.2012.07.021.
34. Song Y, Yang X, Li S, Luo Y, Chang JS, Hu Z. Thraustochytrids as a promising source of fatty acids, carotenoids, and sterols: bioactive compound biosynthesis, and modern biotechnology. Crit Rev Biotechnol 2024;44:618-640.10.1080/07388551.2023.2196373.
35. Jia YL, Du F, Nong FT, Li J, Huang PW, Ma W, et al. Function of the Polyketide synthase domains of Schizochytrium sp. on fatty acid synthesis in Yarrowia Lipolytica. J Agric Food Chem. 2023;71:2446–54. https://doi.org/10.1021/acs.jafc.2c08383.
36. Han X, Zhao Z, Wen Y, Chen Z. Enhancement of docosahexaenoic acid production by overexpression of ATP-citrate lyase and acetyl-CoA carboxylase in Schizochytrium Sp. Biotechnol Biofuels. 2020;13:131. https://doi.org/10.1186/s13068-020-01767-z.
37. Li L, Liu X, Wei K, Lu Y, Jiang W. Synthetic biology approaches for chromosomal integration of genes and pathways in industrial microbial systems. Biotechnol Adv. 2019;37:730–45. https://doi.org/10.1016/j.biotechadv.2019.04.002.
38. Wu XL, Li BZ, Zhang WZ, Song K, Qi H, Dai JB, et al. Genome-wide landscape of position effects on heterogeneous gene expression in Saccharomyces cerevisiae. Biotechnol Biofuels. 2017;10:189. https://doi.org/10.1186/s13068-017-0872-3.
39. Sauer C, Syvertsson S, Bohorquez LC, Cruz R, Harwood CR, van Rij T, et al. Effect of genome position on Heterologous Gene expression in Bacillus subtilis: an unbiased analysis. ACS Synth Biol. 2016;5:942–7. https://doi.org/10.1021/acssynbio.6b00065.
40. Bryant JA, Sellars LE, Busby SJ, Lee DJ. Chromosome position effects on gene expression in Escherichia coli K-12. Nucleic Acids Res. 2014;42:11383–92. https://doi.org/10.1093/nar/gku828.

Publisher's note